JBC Papers in Press. Published on November 1, 2007 as Manuscript M707593200
The latest version is at http://www.jbc.org/cgi/doi/10.1074/jbc.M707593200

Global Disruption of Cell Cycle Progression and Nutrient Response by the Antifungal Agent Amiodarone

Yong-Qiang Zhang and Rajini Rao[#]

From the Department of Physiology, The Johns Hopkins University School of Medicine
725 N. Wolfe Street, Baltimore, MD 21205

Running Title: Transcriptional profiling of amiodarone response in yeast

[#]Address correspondence to: Phone: 410 955 4732; Fax: 410 955 0461; Email: rrao@jhmi.edu

The antiarrhythmic drug amiodarone has fungicidal activity against a broad range of fungi. In *S. cerevisiae*, it elicits an immediate influx of Ca^{2+} followed by mitochondrial fragmentation and eventual cell death. To dissect the mechanism of its toxicity, we assessed the transcriptional response of *S. cerevisiae* to amiodarone by DNA microarray. Consistent with the drug induced calcium burst, more than half of the differentially transcribed genes were induced by high levels of $CaCl_2$. Amiodarone also caused rapid nuclear accumulation of the calcineurin regulated Crz1. The majority of genes induced by amiodarone within 10 minutes were involved in utilization of alternative carbon and nitrogen sources and in mobilizing energy reserves. The similarity to nutrient starvation responses seen in stationary phase cells, rapamycin treatment and late stages of shift to diauxic conditions and nitrogen depletion suggests that amiodarone may interfere with nutrient sensing and regulatory networks. Transcription of a set of nutrient-responsive genes was affected by amiodarone but not $CaCl_2$, indicating that activation of the starvation response was independent of Ca^{2+}. Genes down-regulated by amiodarone were involved in all stages of cell cycle control. A moderate dose of amiodarone temporarily delayed cell cycle progression at G1, S and G2/M phases, with the Swe1-mediated delay in G2/M phase being most prominent in a calcineurin-dependent manner. Overall, the transcriptional responses to amiodarone revealed by this study were found to be distinct from other classes of antifungals, including the azole drugs, pointing towards a novel target pathway in combating fungal pathogenesis.

Fungal infections are a persistent problem, especially in immunocompromised patients undergoing treatment for AIDS, cancer, cystic fibrosis and other diseases. Existing antifungal drugs have limitations in that there are relatively few classes with distinct mode of action; of these, the widely prescribed azole drugs are fungistatic and depend upon a healthy immune system for fungal clearance. The need for new drugs that combat resistance and improve the efficacy of existing antifungals is pressing. Amiodarone has been approved to treat ventricular arrhythmias since 1985. Pharmacological studies have shown its property as a cation channel blocker although it has multiple targets and a complex mechanism. Recent *in vitro* research in unicellular organisms demonstrated its microbicidal activity against a broad range of fungal species (1), bacteria (2), and protozoa (3). In *S. cerevisiae*, it elicits an immediate Ca^{2+} burst (4,5) and subsequently a mitochondrial-mediated cell death program (6). Similarly, 12.5 μM amiodarone elevated cytosolic Ca^{2+} in *Trypansoma cruzi* but not in the host Vero cells (3). Low levels of amiodarone (1-4 μM), within the therapeutic range achieved in patients, were reported to exhibit synergistic fungicidal effects with azole drugs against pathogenic species of fungi (*Candida* and *Cryptococcus*) and protozoa (*Trypanosoma*), suggesting that the drug may be useful as a sensitizing agent in antimicrobial therapy (5).

A comprehensive view of the impact of amiodarone on microbial cellular pathways is prerequisite for its potential *in vivo* use as antifungal adjunct, and to understand mechanisms of drug toxicity and resistance. Phenotypic profiling of the set of *S. cerevisiae* single gene deletions for amiodarone hypersensitivity revealed the importance of genes involved in membrane trafficking and transport pathways, protein fate, and interaction with the cellular environment (5,7).

Extending the analysis to include additional drugs (tunicamycin, sulfometuron methyl, wortmannin) and ion (Ca^{2+}, Mn^{2+}) stress revealed that the major cellular components responsive to drug toxicity and ion stress localize to the endomembrane system. Notably, disruption of calcium and proton homeostasis by deletion of *PMR1* (Golgi Ca^{2+}, Mn^{2+}-ATPase) and *VMA* (endomembrane/ vacuolar H^{+}-ATPase) genes led to multidrug hypersensitivity. Genes involved in ergosterol biogenesis (*ERG6*, *ERG24*), lipid flipping and remodeling (*SAC1*, *LEM3*, *CDC50, OPI1*), and compartmental trafficking (*RIC1*, *COG6*, *VPS20*) were important for growth tolerance to toxic drugs. Together, these represented the first line of defense against diverse forms of toxic stress.

Phenotypic profiling of multidrug sensitivity also pointed to a significant transcriptional response: genes involved in chromatin remodeling (*HAF4*, *SNF5, SNF6, SWI3*), histone modification (*HFI1, GCN5*) and transcription activation (*SUT2, SRB8, SIN4, HCM1, SIP3, SFP1, UGA3*) were important for survival in amiodarone (7). To gain a global perspective on the impact of this drug on gene expression networks, we profiled the genome-wide transcriptional response of *S. cerevisiae* to amiodarone by DNA microarray. Our findings demonstrate a prominent overlap between amiodarone and calcium stress responses, consistent with the drug induced Ca^{2+} burst reported earlier. Unexpectedly, transcriptional profiling revealed that amiodarone appeared to disrupt nutrient sensing and regulatory networks and delay cell cycle progression. In addition to Ca^{2+} stress, both cell cycle block and nutrient starvation may contribute to the antifungal mechanism of amiodarone.

Experimental Procedures

Yeast strains, media and amiodarone treatment conditions

Yeast deletion mutants (*swe1*Δ, *cnb1*Δ, *crz1*Δ), isogenic to BY4742, were from MATα *S. cerevisiae* deletion library (Invitrogen, Carlsbad, CA). Yeast strains were grown in standard synthetic complete (SC) medium or YPD medium at 30ºC. Liquid cultures were incubated at 30ºC with shaking (250 rpm) and growth was determined by absorbance at 600 nm. Amiodarone (Sigma, St. Louis, MO) was added from a stock solution of 50 mM in dimethylsulfoxide to 100 ml log phase culture (OD 0.1, SC medium) to concentrations specified in Figure legends. DMSO was added to 0.03% (v/v) in the control culture. These conditions were used for determination of doubling time, viability, DNA microarray and fluorescent microscopy. To determine cell viability, samples were collected 10 min and 6 h after addition of amiodarone (15 μM) or DMSO and equal numbers of cells for each treatment (determined after reading OD_{600}) were spread on YPD plates, incubated at 30ºC for 36 h before counting 500-1,500 colonies to calculate cell viability.

Microarray hybridization and bioinformatic analysis

S. cerevisiae BY4742 strain was used for DNA microarray experiment. Culture and amiodarone treatment conditions are as described above. The DMSO control samples were collected 10 min after DMSO addition. The amiodarone-treated samples were collected 10 min and 6 h after amiodarone addition. Cells were spun down at 4000 rpm and flash-frozen after removing the supernatant. Two independent samples for each treatment (DMSO control, amiodarone 10 min and 6 h exposure) were collected and analyzed with DNA microarray. Total RNA was isolated by the hot acidic phenol extraction method as previously described (8). RNA concentration and purity were determined spectrophotometrically by measuring absorbance at 260 and 280 nm. The integrity of the RNA samples was confirmed by polyacrylamide gel electrophoresis. cDNA synthesis, labeling and hybridization, image scanning and processing were conducted at the Johns Hopkins Microarray Core Facility. Briefly, first and second strand cDNA was synthesized with Superscript II (Invitrogen) and DNA polymerase I (Invitrogen). Biotin labeled cRNA was synthesized with T7 RNA Polymerase (ENZO Life Sciences, Inc) and fragmented. Sample cocktail was hybridized to Yeast Genome 2.0 Arrays (Affymetrix). The arrays were stained and washed using the Affymetrix GeneChip Fluidics Station 450 and Mini_euk2V3_450 fluidics script. All arrays were scanned in the Affymetrix GeneChip Scanner 3000 and raw analysis performed with Affymetrix GeneChip Operating System (GCOS) 1.4.

Subsequently microarray data were imported to GeneSpring 7.0 (Agilent Technologies) for normalization and analysis. Data for genes showing two-fold or greater response to amiodarone were imported to Gene Cluster 3.0 (9) for hierarchical and k-means clustering analyses, along with previously published DNA microarray data for these genes in response to $CaCl_2$ (10), rapamycin (11), amino acid or nitrogen depletion, growth in YPD (12), diauxic shift (13), and four classes of antifungals (caspofungin, ketoconazole, 5-fluorocytosine, amphotericin B14), downloaded from publisher's website or requested from the authors. Results were displayed with Java Tree View software and edited in Adobe Photoshop (Adobe Systems Inc.). Geneset enrichment analyses were performed on the server at Munich Information center for Protein Sequences (MIPS) database (http://mips.gsf.de/proj/funcatDB/search_main_frame.html).

Quantitative RT-PCR

Aliquots of the same RNA samples used for DNA microarray were saved for quantitative RT-PCR. The RNA samples were treated with DNase I (Roche, Mannheim, Germany) to remove residual genomic DNA. First strand cDNA was synthesized from 1 µg of total RNA with SuperScript III Reverse Transcriptase (Invitrogen, Carlsbad, CA) according to the manufacturer's instructions. Quantitative RT-PCR was conducted with SYBRE GREEN PCR Master Mix in a 7500 Real Time PCR system (Applied Biosystems, Foster City, CA). A dissociation curve was generated at the end of each PCR to verify that a single DNA species was amplified. *ACT1* was amplified as the reference gene to calculate fold change for genes of interest. All quantitative RT-PCR experiments were conducted in triplicate. Data were analyzed with Sequence Detection Software (Applied Biosystems). Fold changes and standard deviations were calculated with the standard curve method according to the manufacturer's instructions.

Fluorescence Microscopy

For microscopy with FUN-1 (Invitrogen, Carlsbad, CA), BY4742 cells were exposed to amiodarone (15 µM) or DMSO for 10 minutes or 6 h, collected by centrifugation and resuspended in 50 µl SC medium with 4 µM FUN-1 dye (diluted from a stock of 200 µM in dimethylsulfoxide). Following incubation at 30ºC for 1 h, cells were examined under a Zeiss Axiophot fluorescence microscope equipped with a Photometrics Coolsnap fx camera. The fluorescent dye was excited by UV light. Conversion of FUN-1 into cylindrical intravacuolar structures was monitored by recording fluorescent micrographs at emission wavelengths of 645 nm (metabolically active and inactive cells) or 525 nm (metabolically inactive cells only). To monitor Crz1p translocation, *crz1*Δ yeast cells expressing GFP-Crz1 from plasmid pKK249 (15) were grown to OD 0.1 and treated with $CaCl_2$ (50 mM) or amiodarone (15 µM) for specified time. Cells were collected by rapid centrifugation and visualized with the Zeiss Axiophot fluorescence microscope at emission wavelength of 525 nm. A total of 300-500 cells were counted for each condition to calculate percentage of cells showing nuclear translocation of Crz1p. Nuclei were stained with 1 µg/ml DAPI (Roche, Mannheim, Germany). Pseudo-colorization was done with Adobe Photoshop.

Flow cytometry and Cell Cycle manipulations

In experiments with asynchronous cultures, amiodarone (15 µM) and FK506 (1 µg/ml) were added to 200 ml BY4742 yeast (OD 0.1) in YPD and samples collected at the specified time intervals. For cell cycle synchronization, 0.2 M hydroxyurea was used to arrest the yeast strains at S phase. The cells were then released into YPD medium for 15 min or 1 h before addition of amiodarone (15 µM). For flow cytometry, cultures were spun down, resuspended in 0.3 ml of 0.2 M Tris-HCl (pH 7.5) buffer and fixed by addition of 0.7 ml of ethanol (95%) at 4ºC for 2 hours. The cells were washed with the above buffer once before treatment with RNase A solution (1 mg/ml in 0.2 M Tris-HCl buffer, pH 7.5) for 2 h at 37ºC. The cells were washed once and stained with 1 µM of SYTOX Green (Invitrogen) in 50 mM Tris-HCl (pH 7.5). Samples (20,000 cells) were analyzed with a FACScan instrument (BD Biosciences). Results were visualized with FlowJo software (Tree Star, Inc, Ashland, OR) and edited with Adobe Photoshop. Distribution of cell population in G1, S and G2/M phases was calculated with FlowJo.

Results

Dose dependent growth inhibition and metabolic arrest by amiodarone

To reveal a substantive transcriptional response to amiodarone without eliciting secondary effects, we sought a drug concentration that would prolong the doubling time of the culture by two-fold. Figure 1A shows that addition of amiodarone to an exponentially growing yeast culture in synthetic complete medium caused a dose dependent inhibition of growth, with a doubling time of 110 minutes in the absence of drug increasing progressively to 150 minutes (9 μM), 170 min (12 μM), 230 min (15 μM) and 380 min (18 μM). Additional amiodarone completely inhibited growth. At 15 μM, amiodarone was moderately fungicidal, with a 19 +/- 2% decrease in colony forming units after a ten-minute exposure to drug. Longer exposure times increased the fungicidal effect, with a loss in colony forming units of 34 +/- 8% after 6 h. Similar effects were seen in cells loaded with the FUN-1 dye (16), that monitors loss of metabolic activity by a change in fluorescence from red cylindrical structures to diffuse green-yellow stain (Figure 1B). Based on these results, we chose to monitor both early (10 minutes) and late (6 h) transcriptional response to a moderate dose of amiodarone (15 μM).

Overview of differentially transcribed genes

Within 10 minutes of exposure to 15 μM amiodarone, we observed differential transcription of 352 genes, using a 2-fold margin as cut-off. Of these, 218 gene transcripts increased, whereas 134 decreased (Table 1S; supplemental data). At 6 h, the response was considerably muted, with 106 genes maintaining ≥ 2-fold increase and only 9 genes remaining at ≥ 2-fold decrease. These data suggest that the transcriptional response reached its peak shortly after drug exposure and diminished over time, consistent with the fungicidal efficacy of the drug. Since this was confirmed using additional time intervals (not shown), we focused our analysis on the transcriptional response at 10 min of drug exposure.

Relative to the yeast proteome, the differentially up-regulated gene products were significantly enriched in functional categories of metabolism (*P* value, 5.66×10^{-6}) and energy production (*P* value, 4.56×10^{-9}), with protein localization predominantly in membranes (plasma membrane and endomembranes) and in peroxisomes, as shown in Figure 2. In contrast, down-regulated genes were highly enriched in functional categories of cell cycle and DNA processing (*P* value, 1.19×10^{-7}), cell type differentiation (*P* value, 1.60×10^{-5}) and cell communication (*P* value, 2.49×10^{-5}). Protein localization of down-regulated gene products showed significant enrichment in the yeast bud and cell periphery, whereas other cell compartments were represented at levels similar to the yeast proteome (Figure 2).

To validate our DNA microarray data, we performed real-time quantitative PCR on 26 genes representing a variety of enriched functional categories. Results from real-time PCR were in good agreement with DNA microarray results (Table 2S; supplemental data), with fold change in transcript levels being similar to, or greater than results from microarray. This indicated that the DNA microarray results faithfully represented the transcriptional response to amiodarone.

Amiodarone triggers a large transcriptional response to Ca^{2+} burst

Among the genes showing differential transcription in response to amiodarone, many are also known to respond to elevation of cytosolic Ca^{2+} (*RCN1*, *ENA1-5*, *CMK1*, *CMK2*, *GYP7*), consistent with the drug induced calcium burst reported previously (4,5). Figure 3A shows that a large percentage of the amiodarone responsive gene set was also induced (137 of 218 genes; 63%) or repressed (77 of 134 genes; 57%) upon exposure to 200 mM $CaCl_2$ (10). A hierarchical clustering analysis confirmed that the transcriptional response to amiodarone most closely resembled the response to high $CaCl_2$ (Figure 4).

The transcription factor Crz1 is the major effector of calcineurin, a highly conserved Ca^{2+}/calmodulin activated protein phosphatase that couples Ca^{2+} signals to downstream responses. Analogous to the NFAT family of transcription factors in mammalian cells, yeast Crz1 is dephosphorylated by calcineurin and migrates to the nucleus where it induces expression of target genes in response to a Ca^{2+} signal. We monitored the intracellular localization of Crz1-GFP upon

exposure to amiodarone (15 μM) and high $CaCl_2$ (50 mM). There was an immediate relocalization of Crz1 to the nucleus upon addition of amiodarone, similar to but more transient than the effect of 50 mM extracellular Ca^{2+} (Figure 3 B-C). Combined with the microarray data, this result demonstrates that amiodarone induced Ca^{2+} influx is capable of mounting a robust downstream transcriptional response.

Amiodarone induces a stress response

Previous studies have identified a number of genes whose expression is altered under stress. In one study, expression of 216 genes was induced in response to seven stress conditions, namely heat, high salt, acid, alkali, H_2O_2, hyperosmolarity and diauxic shift (17). Of these, 54 gene transcripts (Figure 3 A; Table 3S supplemental data) were also induced by amiodarone, mostly as a response to Ca^{2+} stress; fewer (11 genes) were repressed in common with general stress response. Transcription of most (~60%) of these 54 genes is under the control of the *MSN2*/*MSN4* stress regulated factors. This indicates that the cell initiates its defense mechanism to cope with amiodarone toxicity.

Amiodarone induces a unique nutrient starvation response

The majority of amiodarone induced genes were involved in utilization of alternative carbon and nitrogen sources and mobilizing energy reserves (Table 1). This included genes for metabolizing the storage carbohydrates trehalose and glycogen (*TPS2*, *GAC1*, *GLC3*, *GPH1*, *GSY1*, *GSY2*, and others), fermenting non-glucose carbohydrates (*FDH1*, *ACS1*, *ALD4*, *CYB2* and others) and metabolizing fatty acids (*FOX2*, *POX1*, *POT1*, *ECI1, FAA2, CTA1, PXA1, PXA2, IDP3, TES1* and YPL156C). Concomitantly, we observed an induction of transporters for galactose (*GAL2*), maltose (*MAL31*), and high-affinity and moderate-affinity scavengers of glucose (*HXT4*, *HXT5*, *HXT6*). Numerous genes involved in regulating glucose metabolism were up-regulated *(MTH1*, *CAT8*, *REG2*, *NRG1*, and *MIG2*) or repressed (*STD1*, *CYR1*, *SRB8, MIG1* and *GAL11*) upon exposure to amiodarone. Similarly, genes under Nitrogen Catabolite Repression, including *GAP1*, *MEP2*, *DAL80*, *DAL4*, *DAL7*, *PUT1*, *PUT4*, *UGA4*, and *PRB1*, were derepressed. Induction of these genes is triggered by depletion of preferred nitrogen sources such as ammonium and glutamine. Collectively, the pattern of global transcriptional change induced by amiodarone is reminiscent of a starvation response. Indeed, hierarchical clustering analysis demonstrated that the transcriptional response within 10 min of exposure to amiodarone was similar to glucose and nitrogen starvation observed during stationary phase, rapamycin treatment and late stages of diauxic shift and nitrogen depletion (Figure 4A). Thus, the rapid and extensive re-programming of yeast metabolic networks to adapt to nutrient-limiting conditions, despite the availability of glucose and ammonium in the medium, suggests that amiodarone may disrupt nutrient sensing and regulatory circuitry.

Comparison of the transcriptional profiles in response to amiodarone and $CaCl_2$ by K-means clustering revealed a signature response of amiodarone; a cluster of 52 genes was induced at least twofold by amiodarone but not by $CaCl_2$ (Figure 4 B, Table 4S, supplemental data). Of these, 25 genes are known to be activated upon carbon or nitrogen starvation and include key regulators of glucose metabolism (such as *CAT8, MIG2, GAC1, MTH1, REG2*), high affinity glucose transporters (*HXT4, HXT6*), and genes for alternative carbon metabolism (*MAL31, MAL33, POT1, POX1* and others). Additionally, none of the glucose metabolism regulators (*STD1*, *CYR1*, *SRB8, MIG1* and *GAL11*) repressed by amiodarone was repressed by $CaCl_2$ (10). We investigated, by quantitative RT-PCR, the expression of a subset of these genes upon exposure to 200 mM $CaCl_2$: high levels of Ca^{2+} did not affect these nutrient-responsive genes, whereas expression of the calcium-responsive *CMK2* was induced by 24-fold (Table 2S, supplemental data). Together, these data indicate that amiodarone activates a starvation response by a mechanism independent of Ca^{2+} signaling.

Amiodarone blocks cell cycle progression

Genes down-regulated by amiodarone were highly enriched in the category of cell cycle regulation (Table 2). Key cell cycle regulators included *CLB6* (promoting DNA replication), *CLB1* and *CLB2* (promoting nuclear division), *FKH2* (promoting G2/M transition), *SWI5* and *ACE2* (promoting M/G1 transition). In addition,

genes involved in the processes of DNA synthesis and replication, and cytokinesis were repressed. Other important cell cycle regulators, including *CLB3*, *CLB4* and *CLB5*, were also repressed, albeit at lower levels (1.5-2 fold). To investigate if this large-scale repression of cell cycle genes was mediated by Ca^{2+}, we examined the DNA microarray dataset previously reported for calcium response (10). This dataset includes genes repressed by Ca^{2+} (200 mM) that have not been analyzed, to date. Among the 712 genes repressed by Ca^{2+} within 15 min, 114 genes are in the functional category of cell cycle and DNA processing. Of the 43 cell cycle genes repressed by amiodarone, 26 were also repressed by high Ca^{2+}, including all key cell cycle regulators listed above, with the exception of *CLB3* and *CLB4*. Therefore, Ca^{2+} signaling plays a prominent role in mediating repression of the cell cycle genes by amiodarone.

Genes repressed by amiodarone are required to promote progression through all phases of the cell cycle, suggesting that the drug might impose a delay at multiple stages of the cell cycle. To examine this hypothesis, we assessed the effect of amiodarone on the cell cycle by flow cytometry. In an asynchronous early log phase control culture, the cell populations in G1, S, and G2/M phases were 16%, 22% and 60%, respectively. Following treatment with 15 μM amiodarone for 0.5 h, cell populations in G1, S, G2/M phases were 20%, 0 and 80%, respectively. In addition, populations of cells with lower DNA content appeared, indicative of cell death and DNA degradation. Eight hours after amiodarone treatment, the cell cycle profile returned to normal (Figure 5A). These results suggested that the transitions from G1 to S phase and from G2/M to G1 were temporarily blocked. To further assess the blockage of cell cycle at specific stages, we examined the effect of amiodarone in synchronous cultures. Wild type yeast were arrested in S phase with hydroxyurea and released to YPD. Amiodarone was added to the culture during transition from S to G2/M phase (Figure 5B) or from G2/M to G1 phase (Figure 5C). These analyses showed that the transition from S to G2/M phase was temporarily delayed while the transition from G2/M to G1 phase was significantly blocked in the presence of drug.

Elevation of Swe1 kinase activity is required for transient G2/M arrest, by phosphorylation and inhibition of Cdc28, under several conditions including exposure to calcium (in a *zds1*Δ mutant), ER stress, and hyperosmotic stress (18-20). To investigate the role of Swe1 in amiodarone-induced G2/M arrest, we examined cell cycle progression in a *swe1*Δ mutant following synchronization with hydroxyurea treatment and release. In contrast to wild type, *swe1*Δ cells failed to arrest in G2/M phase when treated with 15 μM amiodarone (Figure 6A). Consistent with this, 0.5 h after amiodarone treatment, asynchronous *swe1*Δ mutant culture contained ~10% multinucleate cells while the wild-type culture contained ~2% of multinucleate cells (Figure 6B). Taken together, these results confirmed the role of Swe1 in mediating G2/M arrest and indicated a specific involvement in blocking nuclear division.

Calcineurin is critical for viability in amiodarone and mediates G2/M block

Deletion of calcineurin (*cnb1*Δ) or inhibition by FK506 was previously demonstrated to confer growth hypersensitivity to amiodarone (5). We show that acute inhibition of calcineurin with FK506 increased cell death in amiodarone, as evidenced by accumulation of cells with decreased DNA content (Figure 7A). Furthermore, synchronized *cnb1*Δ cells progressed from G2/M phase to G1 phase in a manner similar to untreated cells, albeit with the appearance of sub-G2/M peaks of cells, likely representing DNA breakdown (Figure 7B). In the absence of amiodarone, neither FK506 nor disruption of *CNB1* had a discernable effect on cell death or cell cycle. Together, these data indicated that calcineurin was involved in mediating the G2/M arrest induced by amiodarone and that in the absence of cell cycle arrest, increased cell death ensued.

Discussion

Mechanistic insights from transcriptional profiling

Amiodarone is a cationic amphiphilic drug that has a strong preference to partition into the membrane bilayer where it has been shown to exert an ordering effect on lipids, resulting in a decrease in membrane fluidity (2,21). In yeast, amiodarone triggers the rapid opening of plasma membrane calcium channels (4,5). Both the

kinetics and amplitude of the Ca^{2+} burst are dose-dependent and correlate directly with drug toxicity (S. Muend and R. Rao, submitted). Yeast mutants defective in Ca^{2+} homeostasis are hypersensitive to the drug (5,7). These observations led to a model in which the antifungal effects of amiodarone are a consequence of Ca^{2+} stress. The results from transcriptional profiling directly support this model: over half of the genes differentially transcribed in response to amiodarone were previously identified in a microarray analysis of the response to high Ca^{2+} (10). Similar to the effect of 50 mM extracellular $CaCl_2$, we showed that amiodarone (15 μM) elicited the rapid relocalization of the calcineurin-responsive transcription factor Crz1 to the nucleus. We conclude that Ca^{2+} is a major effector in mediating amiodarone cytotoxicity.

Several lines of evidence indicate that amiodarone also elicits a unique starvation response. First, upregulated transcripts were enriched in categories of energy and metabolism, the two major functional categories also induced in a genome wide study of glucose limitation (22). Second, amiodarone triggered the derepression of the genes for utilization of alternative carbon sources that would normally be under carbon catabolite repression in the presence of glucose (23-26). Consistent with a major metabolic reorganization, numerous regulatory genes in glucose signaling pathways were differentially transcribed in response to amiodarone. Third, the induction of genes for hexose transporters with moderate to high affinity recapitulated the orderly increase in gene transcript levels for hexose transporters of increasing affinity as the cells attempt to scavenge the remaining glucose during the course of diauxic shift (27). Finally, the increased transcription of genes under nitrogen catabolite repression is normally a response to the depletion of preferred nitrogen sources (ammonium and glutamine) in the growth medium (28-30). Thus, the prominent transcriptional adaptation to starvation that occurs within minutes of drug addition despite a sufficient supply of glucose and ammonium, suggests that amiodarone disrupts nutrient sensing or regulatory networks. A unique set of genes, induced by amiodarone but not by $CaCl_2$, constitutes a signature amiodarone response (Figure 4 B). This includes the genes for glucose metabolism regulation, alternative carbon source utilization and glucose scavengers. Additionally, several glucose regulators repressed by amiodarone were not repressed by $CaCl_2$. Therefore, amiodarone elicits the starvation response by a mechanism independent of Ca^{2+}. Further investigation is required to determine whether activation of the starvation response involves specific signaling pathways, such as cAMP/PKA and AMPK (AMP-activated protein kinase).

In addition to a fungicidal effect, we found that amiodarone also elicited a dose-dependent prolongation of doubling time. Consistent with this, a broad spectrum of cell cycle genes was repressed and flow cytometry analysis confirmed the drug-induced delay in cell cycle progression at G1, S and G2/M phases. Exposure to Ca^{2+} has been reported to arrest cells at G2 phase in a *zds1*Δ mutant background, although in wild type cells, the effect of high calcium on cell cycle is minimal (18). Our examination of the global transcriptional change upon exposure to 200 mM $CaCl_2$ revealed repression of a large number of cell cycle genes including most of those repressed by amiodarone (Figure 4; (10). Therefore, blockage of cell cycle progression by amiodarone can be largely attributed to the Ca^{2+} burst. Furthermore, G2 arrest reported in the *zds1*Δ strain was dependent on calcineurin and Swe1 (18). Likewise, we found that the amiodarone induced G2/M block was largely absent in *cnb1*Δ and *swe1*Δ strains. The cell wall integrity (MAPK) pathway was also found to be required for G2 arrest by Ca^{2+} in the *zds1*Δ mutant (18). In addition, the HOG pathway was also reported to be involved in G2 arrest by hyperosmotic shock (19). It is likely that one or more of these MAP kinase pathways are involved in G2/M arrest induced by amiodarone. In summary, transcriptional profiling suggests that antifungal and growth inhibitory effects of amiodarone appear to be mediated by Ca^{2+} stress, disruption of nutrient sensing/signaling and delay in cell cycle progression.

Relationship between transcriptional and phenotypic profiling

Our recent genome-wide phenotypic screen identified 165 gene deletions resulting in amiodarone hypersensitivity (7). Most of these genes were involved in processes of ion homeostasis, lipid metabolism, and chromatin

remodeling, consistent with the reported effect of amiodarone in disrupting Ca^{2+} homeostasis (5) and membrane lipid organization (3). Interestingly, only 11 of these 165 genes showed significant transcriptional response to amiodarone; furthermore, pathways representing genes identified in the phenotypic screen were not enriched in our microarray data. While appearing paradoxical at first sight, the discrepancy between phenotypic and transcriptional profiling has been previously noted (31-33). Haugen et al. argue that phenotypic profiling interrogates pathways that are upstream of the transcriptional response. Thus, since amiodarone is known to disrupt membrane organization and cellular cation homeostasis, mutants with defects in maintaining membrane integrity, ion homeostasis and mounting a transcriptional response to the drug are hypersensitive to amiodarone. Genes identified by phenotypic screening are likely to be constitutively expressed, activated post-translationally (such as, by phosphorylation or protein/cofactor binding) rather than transcriptionally, and have non-redundant functions. For example, calcineurin is activated by Ca^{2+} to mediate a robust transcriptional response to amiodarone, but does not itself undergo a change in transcript levels. On the other hand, transcriptional profiling samples the downstream response to a cellular perturbation and identifies genes that may collectively, rather than individually, be important for adaptation to stress. A combination of both phenotypic and transcriptional profiling approaches can provide complementary and non-overlapping mechanistic insight into a biological process.

Comparison of amiodarone response to other antifungals

The pathways regulated by amiodarone differ significantly from transcriptional responses to members of the four classes of existing antifungal drugs: azoles (ketoconazole), echinocandins (caspofungin), polyenes (amphotericin B) and pyrimidines (5-fluorocytosine). Comparison of whole genome transcriptional responses of amiodarone and these four antifungals (14) revealed very little overlap (Figure 8). As a member of the azole group that inhibit ergosterol biogenesis, ketoconazole modulates genes involved in lipid biosynthesis and sterol uptake, whereas caspofungin inhibits β-1,3-glucan synthase and triggers the induction of the cell wall integrity pathway. The pore forming compound amphotericin B induces genes for membrane reconstruction, cell stress, cell wall integrity, and phosphate uptake and 5-fluorocytosine elicits expression change for genes involved in DNA synthesis, protein synthesis and DNA damage response.

Our results highlight the pathway of amiodarone and Ca^{2+} stress-mediated cell death as a promising target for antifungal development. Indeed, calcineurin inhibitors have already been shown to act synergistically with azoles and other antifungals (34,35), consistent with our report on the synergy between amiodarone and azoles. In light of this, screening amiodarone derivatives in conjunction with existing drugs provides a promising strategy in the battle against fungal pathogens.

Acknowledgements: This work was supported by a Public Health Service grant from the National Institutes of Allergy and Infectious Disease (R01AI065983). We thank Dr. Ameeta Agarwal for providing formatted gene lists for analysis and Dr. Martha Cyert for GFP-Crz1.

Abbreviations: The abbreviations used are: WT, wild type; SC, synthetic complete; DAPI, 4',6-diamidino-2-phenylindole); DMSO, dimethyl sulfoxide.

Table 1
Zhang & Rao, 2007

Functional Category	**Frequency in amiodarone dataset (%)**	**Genome frequency (%)**	***P* value**
Metabolism (83)	38.0	24.6	5.66E-06
C-compound & carbohydrate metabolism (44)	20.1	8.23	1.24E-08
Fatty acid metabolism (6)	2.75	0.39	0.000148
Energy (37)	16.9	5.98	4.56E-09
Fermentation (non-glucose) (9)	4.12	0.76	3.23E-05
Energy reserve metabolism (9)	4.12	0.91	0.000136
Oxidation of fatty acids (5)	2.29	0.14	6.09E-06
Cellular transport (42)	19.2	16.9	0.197659
Anion transport (5)	2.29	0.42	0.001937
Sugar transport (6)	2.75	0.50	0.000659
Amine / polyamine transport (3)	1.37	0.22	0.012073
Lipid/fatty acid transport (5)	2.29	0.71	0.019083
Drug/toxin transport (5)	2.29	0.63	0.011668
Cell rescue, defense & virulence (28)	12.8	9.03	0.034936
Oxidative stress response (5)	2.29	0.89	0.044778
pH stress response (2)	0.91	0.13	0.030590
Heat shock response (3)	1.37	0.32	0.032343
Catalase reaction (2)	0.91	0.03	0.001259

Enrichment of functional categories for genes up-regulated by amiodarone. 218 genes up-regulated by at least two-fold following 10 min exposure to amiodarone (15 μM) were categorized according to the MIPS Functional Catalogue Database. Significantly enriched categories are listed (*P* value cut-off 0.05). Numbers of genes are in parentheses.

Table 2
Zhang & Rao, 2007

Functional Category	**Frequency in amiodarone dataset (%)**	**Genome frequency (%)**	***P* value**
Cell cycle and DNA processing (43)	33.5	16.4	1.19E-07
DNA synthesis and replication (8)	6.25	2.25	0.007966
Mitotic cell cycle and cell cycle control (29)	22.6	7.27	2.18E-08
Cytokinesis/septum formation (6)	4.68	1.15	0.003477
Transcription			
Transcriptional control (17)	13.2	8.07	0.027626
Protein fate			
Modification by phosphorylation & dephosphorylation (9)	7.03	3.03	0.015387
Cellular communication (16)	12.5	3.81	2.49E-05
Small GTPase mediated signal transduction (9)	7.03	0.94	2.55E-06
Cell type differentiation (24)	18.7	7.37	1.60E-05
Budding, cell polarity & filament formation (17)	13.2	5.1	0.000245
Metabolism			
Regulation of C-compound & carbohydrate metabolism (7)	6.46	2.07	0.001654

Enrichment of functional categories for genes down-regulated by amiodarone. 134 genes down-regulated by at least two-fold following 10 min exposure to amiodarone (15 μM) were categorized according to the MIPS Functional Catalogue Database. Significantly enriched categories are listed (*P* value cut-off 0.05). Numbers of genes are in parentheses.

References

1. Courchesne, W. E. (2002) *J Pharmacol Exp Ther* **300**, 195-199
2. Rosa, S. M., Antunes-Madeira, M. C., Matos, M. J., Jurado, A. S., and Madeira, V. M. (2000) *Biochim Biophys Acta* **1487**, 286-295
3. Benaim, G., Sanders, J. M., Garcia-Marchan, Y., Colina, C., Lira, R., Caldera, A. R., Payares, G., Sanoja, C., Burgos, J. M., Leon-Rossell, A., Concepcion, J. L., Schijman, A. G., Levin, M., Oldfield, E., and Urbina, J. A. (2006) *J Med Chem* **49**, 892-899
4. Courchesne, W. E., and Ozturk, S. (2003) *Mol Microbiol* **47**, 223-234
5. Gupta, S. S., Ton, V. K., Beaudry, V., Rulli, S., Cunningham, K., and Rao, R. (2003) *J Biol Chem* **278**, 28831-28839
6. Pozniakovsky, A. I., Knorre, D. A., Markova, O. V., Hyman, A. A., Skulachev, V. P., and Severin, F. F. (2005) *J Cell Biol* **168**, 257-269
7. Yadav, J., Muend, S., Zhang, Y., and Rao, R. (2007) *Mol Biol Cell* **18**, 1480-1489
8. Schmitt, M. E., Brown, T. A., and Trumpower, B. L. (1990) *Nucleic Acids Res* **18**, 3091-3092
9. de Hoon, M. J., Imoto, S., Nolan, J., and Miyano, S. (2004) *Bioinformatics* **20**, 1453-1454
10. Yoshimoto, H., Saltsman, K., Gasch, A. P., Li, H. X., Ogawa, N., Botstein, D., Brown, P. O., and Cyert, M. S. (2002) *J Biol Chem* **277**, 31079-31088
11. Hardwick, J. S., Kuruvilla, F. G., Tong, J. K., Shamji, A. F., and Schreiber, S. L. (1999) *Proc Natl Acad Sci U S A* **96**, 14866-14870
12. Gasch, A. P., Spellman, P. T., Kao, C. M., Carmel-Harel, O., Eisen, M. B., Storz, G., Botstein, D., and Brown, P. O. (2000) *Mol Biol Cell* **11**, 4241-4257
13. DeRisi, J. L., Iyer, V. R., and Brown, P. O. (1997) *Science* **278**, 680-686
14. Agarwal, A. K., Rogers, P. D., Baerson, S. R., Jacob, M. R., Barker, K. S., Cleary, J. D., Walker, L. A., Nagle, D. G., and Clark, A. M. (2003) *J Biol Chem* **278**, 34998-35015
15. Kafadar, K. A., and Cyert, M. S. (2004) *Eukaryot Cell* **3**, 1147-1153
16. Millard, P. J., Roth, B. L., Thi, H. P., Yue, S. T., and Haugland, R. P. (1997) *Appl Environ Microbiol* **63**, 2897-2905
17. Causton, H. C., Ren, B., Koh, S. S., Harbison, C. T., Kanin, E., Jennings, E. G., Lee, T. I., True, H. L., Lander, E. S., and Young, R. A. (2001) *Mol Biol Cell* **12**, 323-337
18. Mizunuma, M., Hirata, D., Miyahara, K., Tsuchiya, E., and Miyakawa, T. (1998) *Nature* **392**, 303-306
19. Alexander, M. R., Tyers, M., Perret, M., Craig, B. M., Fang, K. S., and Gustin, M. C. (2001) *Mol Biol Cell* **12**, 53-62
20. Bonilla, M., and Cunningham, K. W. (2003) *Mol Biol Cell* **14**, 4296-4305
21. Antunes-Madeira, M. C., Videira, R. A., Kluppel, M. L., and Madeira, V. V. (1995) *Int J Cardiol* **48**, 211-218
22. Wu, J., Zhang, N., Hayes, A., Panoutsopoulou, K., and Oliver, S. G. (2004) *Proc Natl Acad Sci U S A* **101**, 3148-3153
23. Schuller, H. J. (2003) *Curr Genet* **43**, 139-160
24. Boer, V. M., de Winde, J. H., Pronk, J. T., and Piper, M. D. (2003) *J Biol Chem* **278**, 3265-3274
25. Rolland, F., Winderickx, J., and Thevelein, J. M. (2002) *FEMS Yeast Res* **2**, 183-201
26. Santangelo, G. M. (2006) *Microbiol Mol Biol Rev* **70**, 253-282
27. Brauer, M. J., Saldanha, A. J., Dolinski, K., and Botstein, D. (2005) *Mol Biol Cell* **16**, 2503-2517
28. Magasanik, B., and Kaiser, C. A. (2002) *Gene* **290**, 1-18
29. Marzluf, G. A. (1997) *Microbiol Mol Biol Rev* **61**, 17-32
30. Cooper, T. G. (2002) *FEMS Microbiol Rev* **26**, 223-238
31. Birrell, G. W., Brown, J. A., Wu, H. I., Giaever, G., Chu, A. M., Davis, R. W., and Brown, J. M. (2002) *Proc Natl Acad Sci U S A* **99**, 8778-8783
32. Begley, T. J., Rosenbach, A. S., Ideker, T., and Samson, L. D. (2002) *Mol Cancer Res* **1**, 103-112

33. Haugen, A. C., Kelley, R., Collins, J. B., Tucker, C. J., Deng, C., Afshari, C. A., Brown, J. M., Ideker, T., and Van Houten, B. (2004) *Genome Biol* **5**, R95
34. Onyewu, C., Eads, E., Schell, W. A., Perfect, J. R., Ullmann, Y., Kaufman, G., Horwitz, B. A., Berdicevsky, I., and Heitman, J. (2007) *Antimicrob Agents Chemother*
35. Steinbach, W. J., Reedy, J. L., Cramer, R. A., Jr., Perfect, J. R., and Heitman, J. (2007) *Nat Rev Microbiol* **5**, 418-430
36. Saldanha, A. J. (2004) *Bioinformatics* **20**, 3246-3248

Figure Legends

Figure 1. *Growth and metabolic effects of amiodarone*. Amiodarone was added to log phase (OD 0.1) cultures of yeast in SC medium at the indicated concentrations. Control cultures contained DMSO (0.03% v/v). *A*. Cell growth was monitored by measuring absorbance at 600 nm in cultures incubated at 30°C for 6 h. *B*. Cells were stained with 4 μM FUN-1 to examine metabolic activity as described under *Experimental Procedures*. Cells showing cylindrical spindle shaped structures (*red*) are metabolically active, whereas cells showing diffuse stains (*red* and *green*) are metabolically inactive.

Figure 2. *Distribution of differentially transcribed genes.* Genes showing two-fold or greater increase (*up-regulated*) or decrease (*down-regulated*) in response to amiodarone (15 μM, 10 min) were grouped in functional categories (*A*) and cellular compartments (*B*) according to the MIPS database. Categories and compartments that are significantly enriched (*P* value < 0.01) relative to the yeast genome are marked with the symbol *.

Figure 3. *Amiodarone triggers a large transcriptional response to Ca^{2+} burst.* (A) Genes induced or repressed by amiodarone (10 min) overlapped markedly with those induced or repressed by Ca^{2+} (5 and 15 min, (10)), respectively. 54 genes induced by amiodarone were previously identified as general stress response genes (17). (B) Fluorescence images of *crz1*Δ strain expressing GFP-Crz1. Cells were visualized immediately after $CaCl_2$ (50 mM) or amiodarone (15 μM) addition. Nuclei were stained with DAPI (1 μg/ml). (C) Distribution (in percentage) of cells scored as nuclear or cytoplasmic for GFP-Crz1 localization. 300-500 cells were counted for each condition.

Figure 4. *Amiodarone elicits a starvation response by a mechanism independent of Ca^{2+}*. (*A*) Hierarchical clustering of 343 genes that were up- or down-regulated by at least two-fold when exposed to 15 μM amiodarone for 10 min. Other transcriptionally regulated genes included in this analysis were downloaded from the publishers' websites or requested from the authors: exposure to $CaCl_2$ (5, 15 and 30 min), rapamycin (30 min), time course series for diauxic shift (successive samples 1-7 were collected between 9 - 20.5 h growth), amino acid starvation (0.5 - 6 h), nitrogen depletion (1 h - 5 days), and growth in YPD (2 h - 5 days). Fold change values under each condition were $\log_2$ transformed and clustered with Gene Cluster 3.0 (9). Distances between genes and arrays were computed based on correlation (centered). Both genes and arrays were clustered with average linkage method. The data were visualized with Java Tree View (36). (*B*) K-means clustering of 343 genes that were differentially regulated by at least two-fold when exposed to 15 μM amiodarone for 10 min. Euclidean distance method was used to calculate similarity matrix. The set of 52 genes induced by amiodarone but not by Ca^{2+} is listed.

Figure 5. *Amiodarone delays cell cycle progression.* Total DNA content was assessed by flow cytometry analysis and presented as cell counts (y-axis) versus DNA content (x-axis; *arrows* indicate IC and 2C). (A) Early log phase culture (OD 0.1) of the wild type (BY4742) was treated with amiodarone (15 μM) for eight hours. 0 time point is the sample before addition of amiodarone. (B) Early log phase culture of the wild type (BY4742) was synchronized at S phase by 0.2 M hydroxyurea for 1 h and then released to YPD

for 15 min for recovery. A sample was collected and analyzed as the 0 time point. The remaining culture was split into two parts. One part was treated with DMSO while the other with amiodarone (15 μM). (C) The culture was synchronized as above and then released to YPD for 60 min for the cells to pass through S phase. A sample was collected and analyzed as the 0 time point. The remaining culture was treated with DMSO or amiodarone as in (B).

Figure 6. *Swe1 is involved in mediating G2/M delay caused by amiodarone.* (A) Early log phase (OD 0.1) culture of the *swe1*Δ strain was synchronized at S phase by 0.2 M hydroxyurea for 1 h and then released to YPD for 60 min for the cells to pass through S phase. Samples were treated as described for Figure 5. (B) Percentage of multi-nucleate cells in WT and *swe1*Δ cultures treated with amiodarone (15 μM). Samples at 0 time point were collected before adding amiodarone. Nuclei were stained with DAPI (1 μg/ml) and 100 - 400 cells were counted to calculate percentage.

Figure 7. *Calcineurin confers protection against amiodarone and mediates G2/M delay.* Early log phase (OD 0.1) culture of wild type (BY4742) was treated with FK506 (1 μg/ml) for 15 min. A sample was collected as the 0 time point. The remaining culture was split into two parts. One part was treated with DMSO while the other with amiodarone (15 μM). (B) Early log phase (OD 0.1) culture of the *cnb1*Δ strain was synchronized at S phase by 0.2 M hydroxyurea for 1 h and then released to YPD for 60 min for the cells to pass through S phase. The culture was then split into two parts. One part was treated with DMSO while the other with amiodarone (15 μM).

Figure 8. *Transcriptional response to amiodarone is distinct from those to other antifungals.* Hierarchical clustering of 1977 genes that were differentially regulated by at least two-fold in one or more of the six conditions shown. Gene expression data for $CaCl_2$ (10) and antifungals (14) were previously published: exposure to $CaCl_2$ (5, 15 and 30 min), caspofungin (~3 h), amphotericin B (~3 h), 5-fluorocytosine (~3 h), ketoconazole (~3 h). Clustering method is the same as that described for Figure 4 A.

Figure 1
Zhang and Rao, 2007

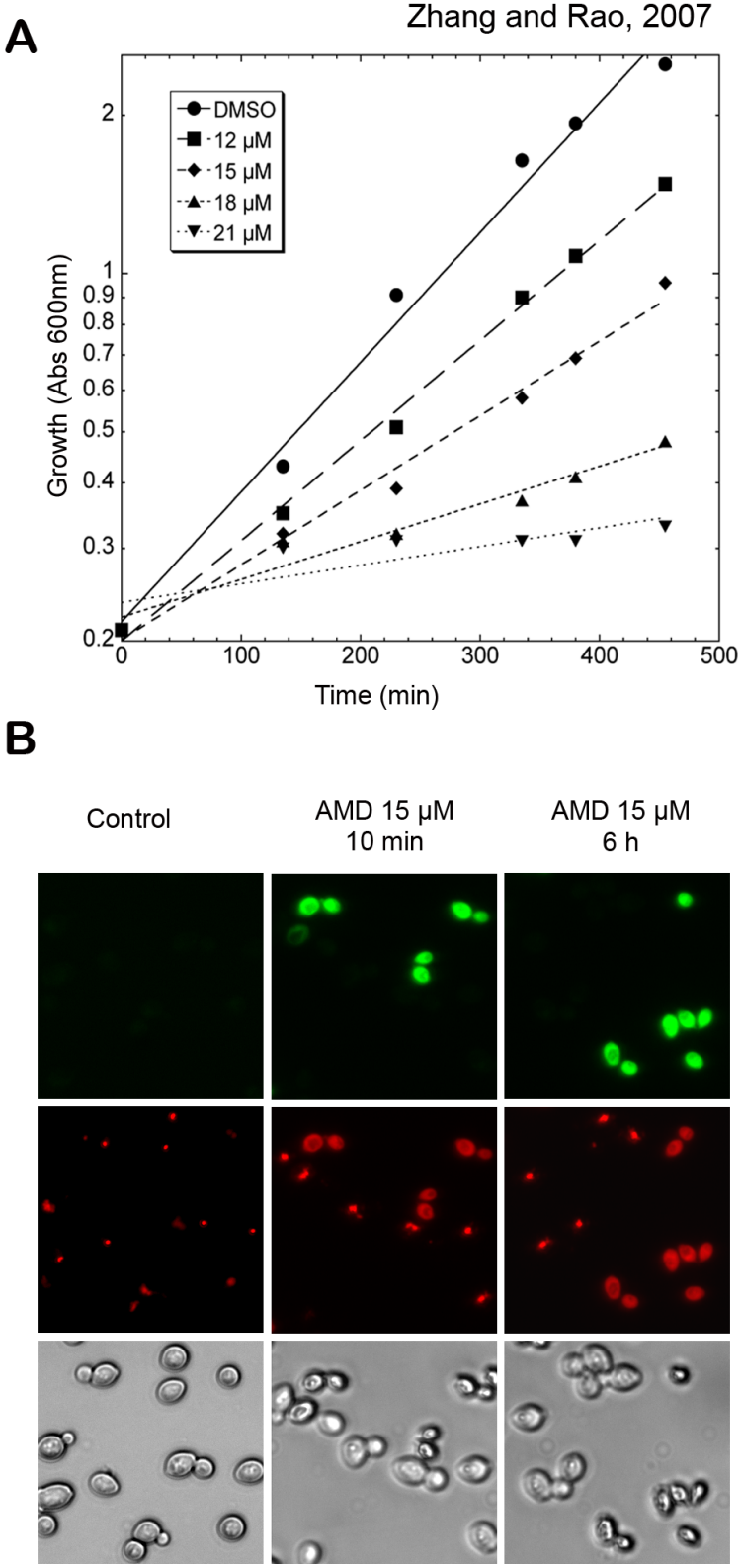

Figure 2
Zhang and Rao, 2007

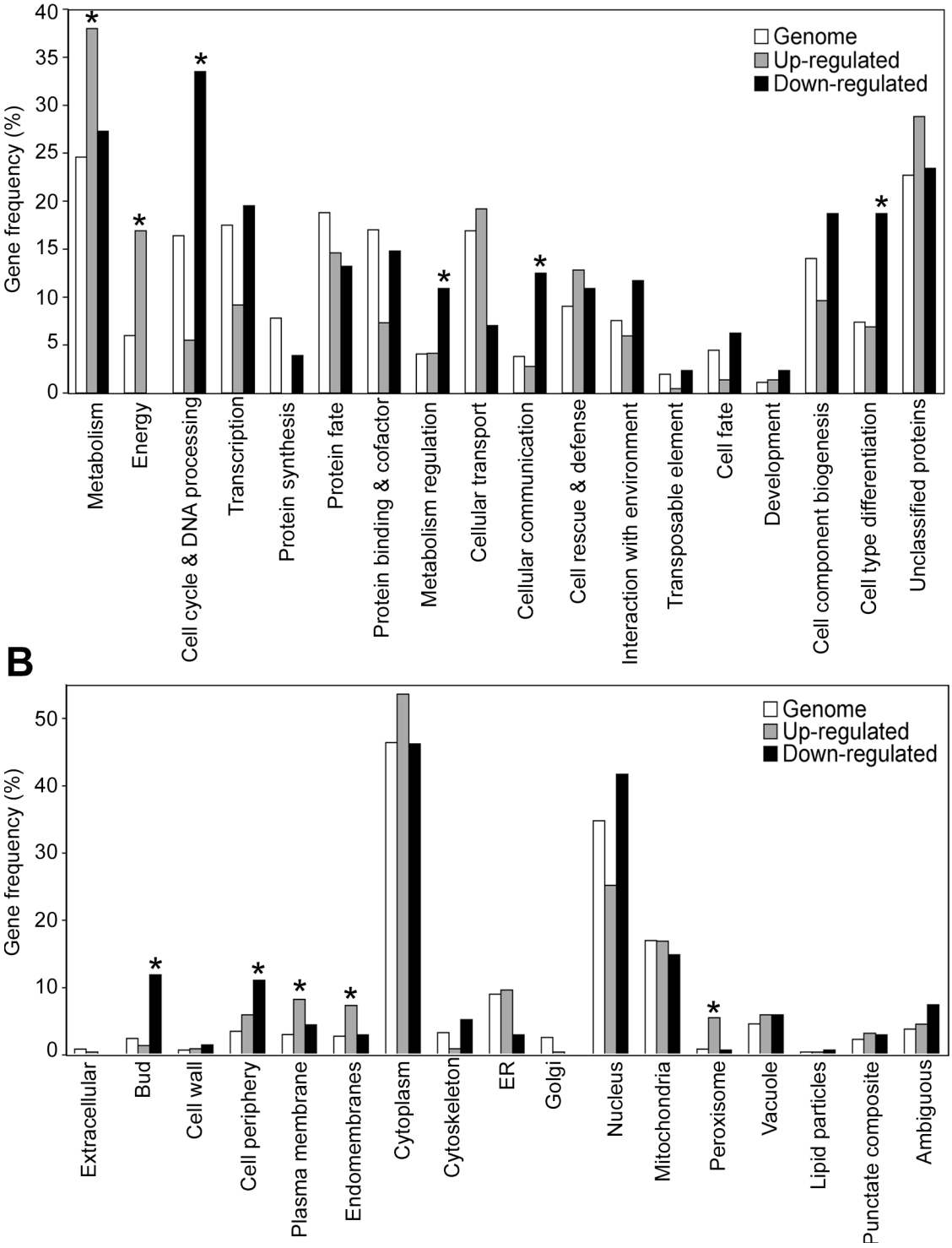

Figure 3
Zhang and Rao, 2007

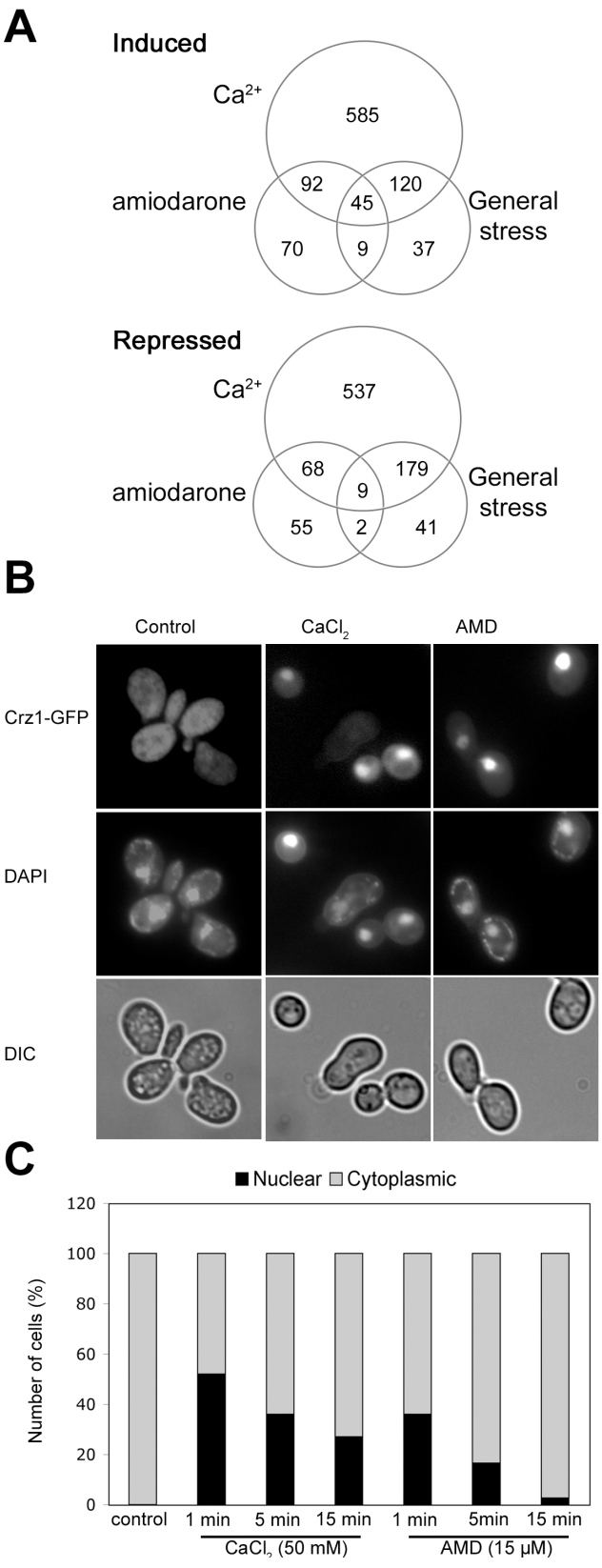

Figure 4
Zhang and Rao, 2007

Figure 5
Zhang and Rao 2007

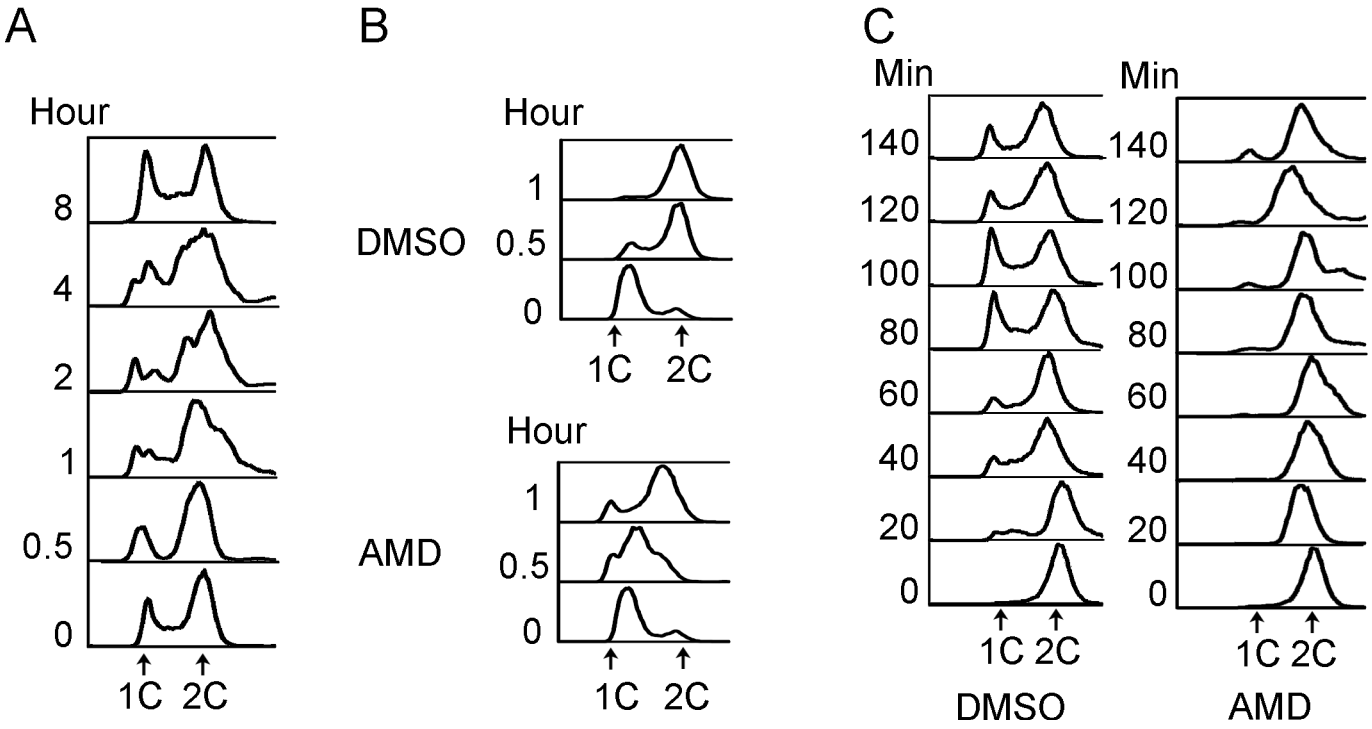

Figure 6
Zhang and Rao 2007

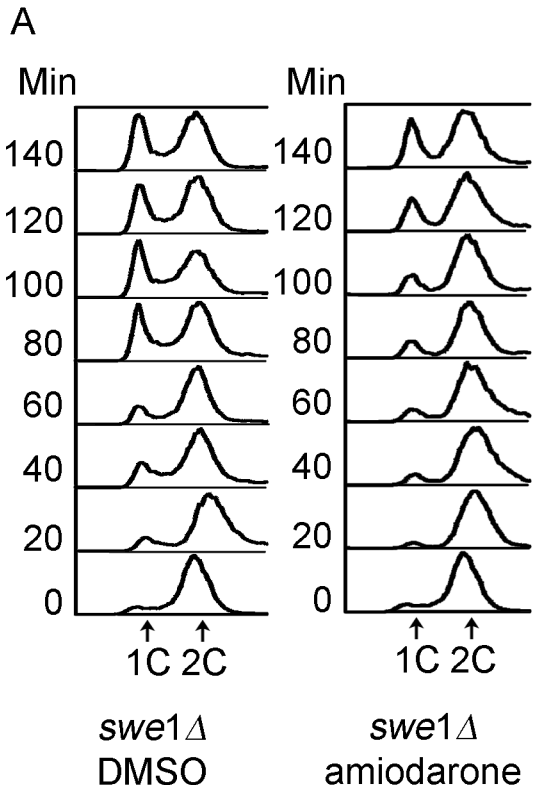

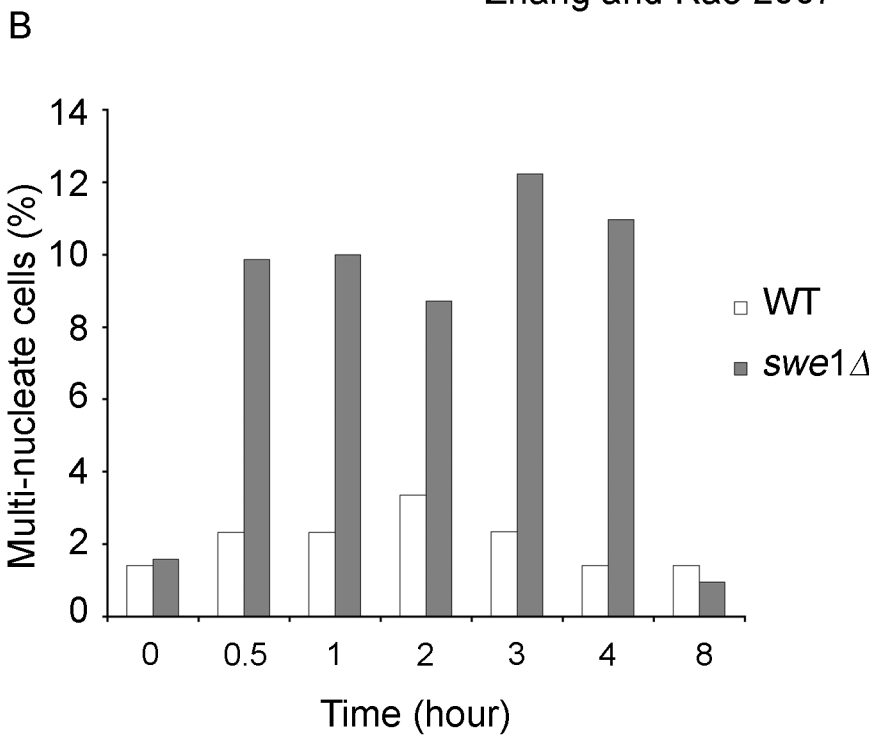

Figure 7
Zhang and Rao, 2007

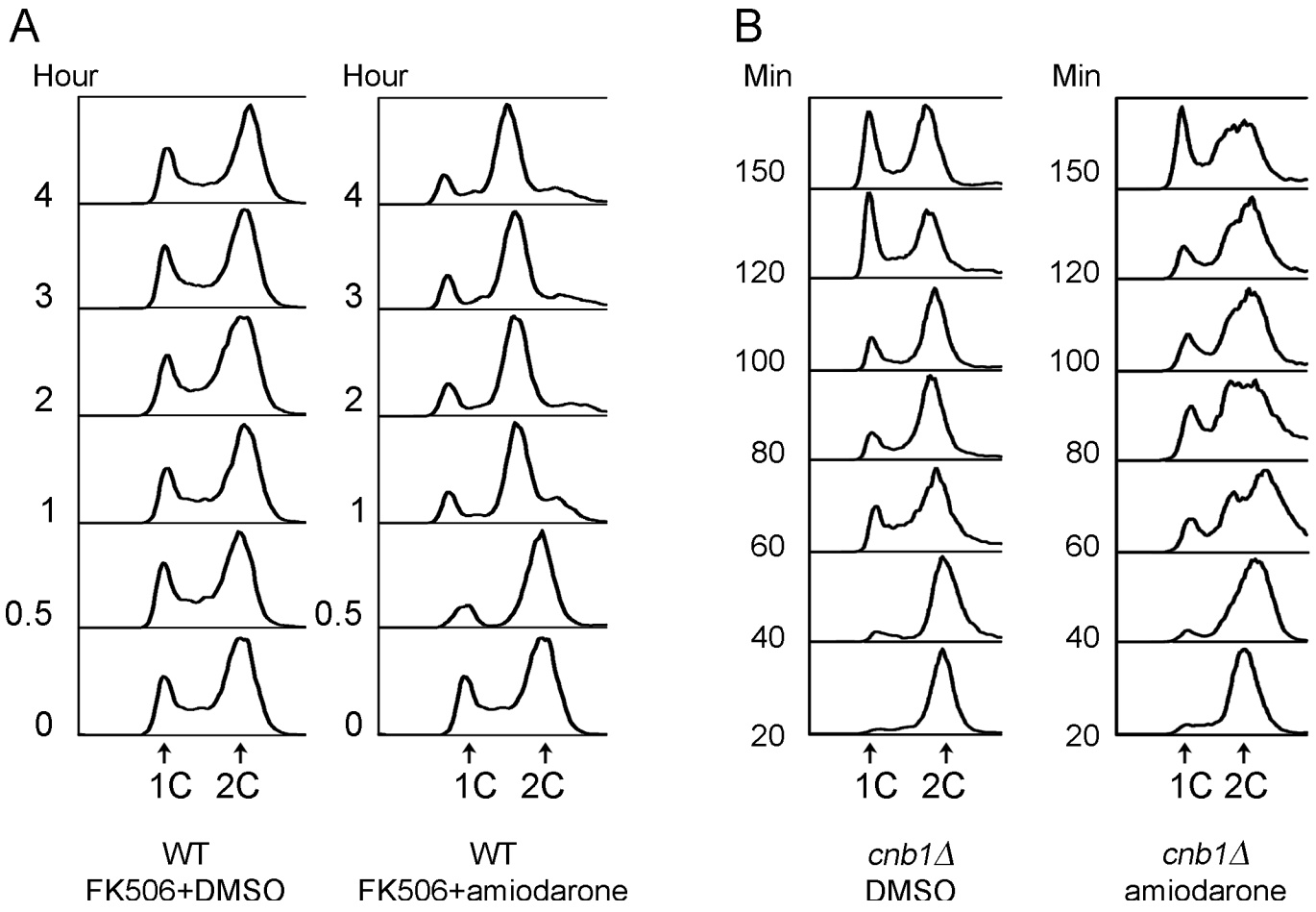

Figure 8

Zhang and Rao, 2007